Clinical Neurophysiology xxx (2013) xxx–xxx

Contents lists available at SciVerse ScienceDirect

Clinical Neurophysiology

journal homepage: www.elsevier.com/locate/clinph

Global organization of functional brain connectivity in methamphetamine abusers

Mehran Ahmadlou [a,b,*], Khodabakhsh Ahmadi [c], Majid Rezazade [d], Esfandiar Azad-Marzabadi [c]

[a] Netherlands Institute for Neuroscience, Amsterdam, The Netherlands
[b] Dynamic Brain Research Institute, Tehran, Iran
[c] Behavioral Sciences Research Center, Baqiyatallah University of Medical Sciences, Tehran, Iran
[d] Aids Prevention & Control Committee of Welfare Organization State, Tehran, Iran

ARTICLE INFO

Article history:
Accepted 7 December 2012
Available online xxxx

Keywords:
Coherence
EEG
Functional connectivity
Methamphetamine
Small-World Network
Visibility graph similarity

HIGHLIGHTS

- This is the first study on the effects of methamphetamine on the global organization of functional brain connectivity.
- The normal Small-World brain network is disrupted at the gamma band in chronic methamphetamine abusers.
- The global network deficit at gamma in methamphetamine abusers may imply on effects of the disrupted dopaminergic system on fast-spiking interneurons.

ABSTRACT

Objective: This study aimed to determine effects of chronic methamphetamine (MA) abuse on global organization of the functional brain connectivity.
Methods: Eyes-closed resting-state EEGs of 36 MA abusers and 36 age-matched healthy subjects were recorded using a 32-channel system. The EEGs (1–60 Hz), after removing artifacts, were decomposed into the conventional EEG bands. Using visibility graph similarity (VGS) and coherence methods, the VGS and coherence matrices in each EEG band were constructed. Then the Small-World Network properties, clustering coefficient (C), mean path length (L) and C/L, of the VGS and coherence matrices, were computed in all EEG bands. Then using the Mann–Whitney test and an artificial neural network the differences of C, L and C/L between the two groups were evaluated.
Results: The MA abusers showed higher C, lower L and higher C/L at the gamma band (p-value <0.005). An accuracy of 82.8% in discriminating the two groups was obtained by the classifier.
Conclusions: The topology of the functional brain connectivity is disrupted in MA abusers, as depicted by deviation from Small-Worldness in the gamma band.
Significance: This is the first but quasi-experimental study showing disrupted topology of the functional brain networks in MA abusers.

1. Introduction

Methamphetamine (MA) is a highly addictive neuro-toxic and psycho-stimulant drug affecting the brain structurally and functionally (Belcher et al., 2009; Tobias et al., 2010; Iudicello et al., 2012). Compared with other addictive stimulants, MA is relatively inexpensive and easily synthesised (Newton et al., 2003; Kalechstein et al., 2009), with substantially high risk of psychotic disorders (for the MA abusers) and a significant impact on public health (Glasner-Edwards et al., 2008; Henry et al., 2010). Also compared to opiate dependence, MA dependence causes greater impairment of cognitive functions (Feil et al., 2010). Moreover, the prevalence of MA use and abuse has increased over the past two decades (Polesskaya et al., 2011; Maxwell and Brecht, 2011). However, only a relatively small number of studies have investigated the effects of MA on the human brain (Feil et al., 2010).

Decreased cerebral blood flow (Polesskaya et al., 2011), increased severity of white matter hyper-intensity signals (Bae et al., 2006), decreased grey matter density in bilateral insula and left middle frontal gyrus (Schwartz et al., 2010), reduced hippocampal volume (Thompson et al., 2004) and abnormalities in regional glucose metabolism (Belcher et al., 2009) are the main MA abuse effects on the human brain observed in imaging studies. The effects of the MA abuse on brain electrical activity have been reported also in some, but few, studies.

* Corresponding author at: Netherlands Institute for Neuroscience, Amsterdam, The Netherlands. Tel.: +31 613750152; fax: +98 2188790869.
E-mail addresses: m.ahmadlou@nin.knaw.nl, mehranahmadlou@gmail.com (M. Ahmadlou).

1388-2457/$36.00 © 2012 International Federation of Clinical Neurophysiology. Published by Elsevier Ireland Ltd. All rights reserved.
http://dx.doi.org/10.1016/j.clinph.2012.12.003

Newton et al. (2003) compared eyes-closed resting state EEGs of 11 MA abusers (with 4 days' abstinence) and 11 normal subjects. They analysed the EEGs between 0.5 and 20 Hz and observed increased EEG power at the delta and theta bands in the MA abusers, compared to the normal subjects. Another study of resting state EEGs (0.5–20 Hz), including nine MA abusers and 10 normal subjects, reported a correlation between theta power and episodic memory performance in the MA abusers (Newton et al., 2004). Some differences in the temporal dynamics of the EEGs (revealed by ERP analysis) also have been shown between the normal subjects and the MA abusers, indicating cognitive deficits in the MA abusers (Nordahl et al., 2003; Silber et al., 2012).

Functional connectivity (FC) has an essential role in information transmission among brain networks, accomplishing cognitive tasks and consequently in everyday life. However, the effects of MA abuse on the FC brain networks have not been studied yet. In this study, using resting state EEGs, the changes of the global organization of the FC in the MA abusers are investigated in the light of the Small-World Network (SWN) concept. SWN is defined as a network with optimum balance between local and global structural characteristics (Watts and Strogatz, 1998). The SWN is characterised by co-existence of dense clustering of connections, needed for segregation, and short path lengths among the network units, needed for integration (Watts and Strogatz, 1998; Sporns and Zwi, 2004; Bassett, 2006). Compared with the other structures such as random and ordered networks, the SWN possesses higher synchronisability and higher speed of information transmission among its units. There are strong evidences showing that the normal neocortex and different brain regions have the SWN structure (Sporns and Zwi, 2004; Bassett, 2006; Park et al., 2008; Sporns et al., 2004; Yu et al., 2008). In many neuropsychiatric and neurologic disorders, the deficient SWN brain has been observed: attention deficit/hyperactivity disorder (Ahmadlou et al., 2012a,b), major depressive disorder (Zhang et al., 2011), Alzheimer's disease (Wang et al., in press), schizophrenia (Liu et al., 2008; Ma et al., 2012) and heroin abuse (Yuan et al., 2010).

This article analyses the SWN properties of the FC brain networks of MA abusers, at different EEG sub-bands, with the purpose of discovering how MA abuse affects the topology of the FC brain network.

2. Method

2.1. Subjects

Thirty-six healthy adults and 36 MA abusers, ranged in age from 20 to 48 years and from 21 to 47 years, respectively, were included in this study. All subjects were male and right handed. The healthy subjects were selected from Tehran citizens informed by oral/written announcements/posters and participated voluntarily. Four healthy subjects had smoked cigarettes in the past and five were current cigarette smokers. They had no history of alcohol/substance abuse according to their self-reports.

The MA addicts were recruited from Narcotics Anonymous (NA) camps of Rebirth Charity Society, Tehran, Iran, in which patients have no access to any illicit substance/drug and also random urine drug screens are routinely employed. The subjects were abstinent from MA and any illicit substance for a period between 1 and 3 weeks. However, they were allowed to smoke cigarettes. MA dependence could be diagnosed, for all users, according to the Diagnostic and Statistical Manual of Mental Disorders, Fourth Edition, (DSM-IV) criteria. MA was the predominant substance as the patients had used it regularly at least 3 times a week, although they had a little and irregular use (but <1 year) of the other substances, heroin, opium, methadone and morphine. Prior to EEG recording, a urine screen was obtained for amphetamines, methadone and opiates, in order to ensure that they had not consumed any illicit drugs. Self-reported histories of MA and other drugs, daily dose, age of onset, lifetime use and nicotine and number of cigarettes smoked per day, were written down by the subjects. MA subjects had used the drug for at least for 2 years with a mean lifetime use of 6.42 years and the mean daily MA dose was 1.02 g. The mean daily MA dose (g/day) normalised by body weight (kg) was 0.013.

The study was approved by the Research Ethics Board of the Baqiyatallah University of Medical Sciences. All subjects signed a written informed consent prior to participation. All of them met the inclusion criteria of the study: no previous mental illness and brain seizure, no psychotropic medication, no alcohol and right handedness. For the healthy subjects, substance abuse was also an exclusion criterion. Right-handedness was assessed by the Edinburgh handedness questionnaire, (range from 0 to 100 for right-handedness). Anxiety, depression and stress severity of all subjects were scored by the Beck Anxiety Inventory (BAI) (range 0–63) and Beck Depression Inventory-II (BDI-II) (range 0–63) and the short form of Depression Anxiety Stress Scales (DASS-21) (range of stress: 0–42), respectively. All subjects had normal general intelligence as they scored >90 by Raven's Standard Progressive Matrices (Raven, 2000). The demographic characteristics of the entire sample are presented in Table 1. Further, personality characteristics, attention, working memory and event-related potentials (ERPs) of the subjects were evaluated for another research project.

2.2. EEG recording

EEGs were recorded using a 32-channel EEG data acquisition system with a sampling rate of 250 Hz and frequency range of

Table 1
Demographic characteristics of the subjects participated in this study.

	Healthy subjects M (S)	MA abusers M (S)	*F*	*p*-Value
Handedness	81.56 (14.22), *N* = 36	93.66 (9.72), *N* = 36	7.5	0.010*
Age (year)	32.68 (6.77), *N* = 36	31.68 (8.76), *N* = 36	0.1	0.721
Body weight (kg)	77.25 (8.25), *N* = 36	77.66 (10.79), *N* = 36	0.0	0.904
General intelligence	118.13 (4.67), *N* = 36	113.08 (7.62), *N* = 36	4.5	0.044*
Stress	6.33 (5.36), *N* = 36	14.28 (6.99), *N* = 36	11.9	0.002**
Depression	8.26 (7.88), *N* = 36	17.71 (11.55), *N* = 36	6.7	0.015*
Anxiety	8.80 (8.23), *N* = 36	14.46 (10.74), *N* = 36	2.6	0.116
Daily nicotine dose (cigarette/day)	2.75 (1.78), *N* = 9	16.71 (4.34), *N* = 36	53.6	0.000**
Lifetime nicotine use (year)	8.16 (8.75), *N* = 9	11.85 (6.09), *N* = 36	0.8	0.390
Daily MA dose (g/day)	–	1.02 (0.80), *N* = 36	–	–
Daily MA dose/body weight	–	0.013 (0.011), *N* = 36	–	–
Lifetime MA use (year)	–	6.42 (3.13), *N* = 36	–	–

N, number of subjects; M, mean; S, standard deviation; MA, methamphetamine.
* *p*-Value less than 0.05.
** *p*-Value less than 0.01.

Please cite this article in press as: Ahmadlou M et al. Global organization of functional brain connectivity in methamphetamine abusers. Clin Neurophysiol (2013), http://dx.doi.org/10.1016/j.clinph.2012.12.003

0.1–100 Hz (and digitised in 16 bits). Using an electrocap, the Ag/AgCl electrodes were placed at 31 scalp locations (Fp1, Fp2, F3, F4, FC3, FC4, C3, C4, CP3, CP4, P3, P4, O1, O2, F7, F8, FT7, FT8, T3, T4, TP7, TP8, T5, T6, Fpz, Fz, FCz, Cz, CPz, Pz and Oz) according to the international 10-20 system. Linked earlobes were used as reference. As combing the scalp effectively decreases scalp–electrode impedance (Mahajan and McArthur, 2010), the scalp of each subject was combed before the EEG recording. The impedance between each electrode and the scalp was monitored for each subject before data collection to be kept below 5 kΩ. The vertical and horizontal electro-oculo-grams (EOGs) were registered on the right eye as well. The EEGs were recorded in 180 s when the subjects were in eyes-closed resting state, sitting on a comfortable fixed chair in a dim and acoustically damped room. An interval of 20,000 data points (80 s) of each participant's EEG judged to be free from eye blinking and EOG artefacts (where absolute amplitude of EOG <70 μV) and free from movement artefacts (based on visual inspection) was selected to be included in the study.

2.3. EEG analysis

Low- and high-pass Butterworth filters with cut-offs of 60 and 1 Hz, respectively, were applied to the EEGs to limit them in the frequency range of 1–60 Hz. Using a 50-Hz notch-filter, the electricity line noise was removed.

An orthogonal Hjorth's method, which is a conventional Laplacian source derivation method, was used for spatial enhancement of the EEGs (Hjorth, 1975; Tandonnet et al., 2005). Therefore, the spatially enhanced EEGs were used for further analysis.

As EEG is intrinsically non-stationary and wavelet analysis is more adapted to the non-stationary signals, compared with the common Fourier transform, it was used for EEG sub-banding in this study. Using a five-level wavelet filter bank, the EEGs were decomposed to the conventional EEG sub-bands: delta (1–4 Hz), theta (4–8 Hz), alpha (8–15 Hz), beta (15–30 Hz) and gamma (30–60 Hz). The mother-wavelet of Daubechies with order of 10 was used for the decomposition. The block diagram of the wavelet decomposition as well as a more detailed description of the procedure has been presented in Ahmadlou and Adeli (2010a).

As the brain is a highly complex and nonlinear system of a huge number of nonlinearly interacted neuronal areas (Mamashli et al., 2010; Ahmadlou et al., 2012d), measuring FC in the brain networks may be conceptually more close to the nonlinear nature of the brain, compared with using linear measures such as the cross-correlation function or coherence (Ahmadlou et al., 2012e). Recently, Ahmadlou and Adeli (2012), proposed a nonlinear synchronization measure, called visibility graph similarity (VGS). The VGS measures generalised synchronization (i.e., when the coupled systems (or one of them) affect each other by sharing their states) among the coupled sub-units (here the sub-units are neuronal areas), based on similarity of their temporal dynamics (Ahmadlou et al., 2012c). The algorithm is briefly presented in Appendix A.

Therefore, using VGS the FC of each pair loci was obtained in each EEG sub-band. Then, at each sub-band a VGS matrix was constructed with the obtained VGS values between signals of all pairwise combinations of the channels. For comparison, the functional brain connectivity in the sub-bands was also obtained through the magnitude square coherence method (Carter et al., 1973; Dauwels et al., 2010). Coherence is a function to measure the linear correlation between coupled systems (which here are the neuronal areas), but in the frequency domain. Therefore by averaging the coherence values over all the frequencies in the range of each EEG band, the coherence matrices in the all EEG sub-bands (delta, theta, alpha, beta and gamma) were obtained. The algorithm is briefly presented in Appendix B.

In graph theory, a graph contains some nodes and edges (connectivity) connecting the pair nodes. A graph is characterised by its adjacency matrix. The adjacency matrix contains values of connectivity between each pair nodes of the graph. Therefore, in a graph-theoretical view, each VGS or coherence matrix is indeed the adjacency matrix of a functional brain connectivity graph (where the nodes are the brain loci and the edges are the associated connectivity between the pair loci) (Ahmadlou and Adeli, 2011). Hence having the VGS and coherence matrices of the sub-bands, the associated graphs were produced. Fig. 1 demonstrates the procedure of transformation of an example 31-channel EEG set (Fig. 1a) into its connectivity graph (Fig. 1c). Connectivity coef-

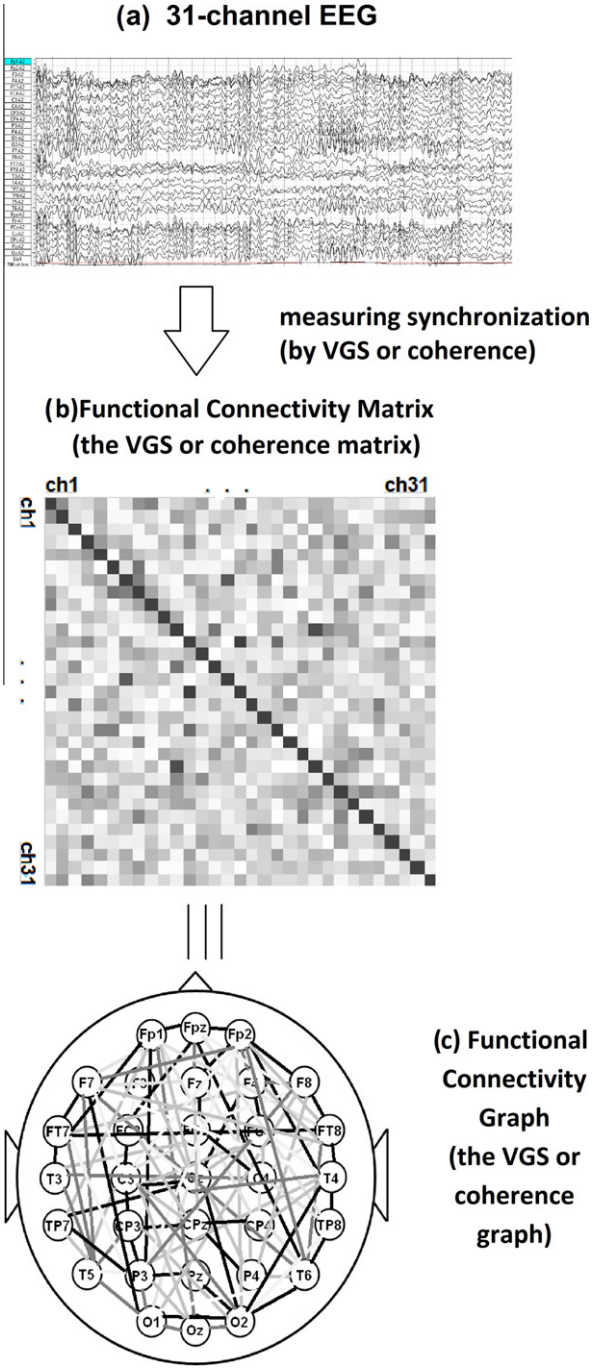

Fig. 1. Illustration of the conversion procedure of a 31-channel EEG to its functional connectivity graph (the VGS or coherence graph).

Please cite this article in press as: Ahmadlou M et al. Global organization of functional brain connectivity in methamphetamine abusers. Clin Neurophysiol (2013), http://dx.doi.org/10.1016/j.clinph.2012.12.003

ficients between channel pairs are calculated and placed in the arrays (squares) of a 31×31 connectivity matrix (Fig. 1b). The light intensity of each array shows the strength of the connectivity. The darker intensity shows a greater value in the connectivity matrix, which corresponds to a darker edge in the connectivity graph (Fig. 1c) (Ahmadlou and Adeli, 2011).

Small-Worldness (SW) of a network is assessed by two characteristics: high clustering coefficient (C) needed for segregation and low mean path lengths (L) needed for integration. The balance between the segregation and integration in a network facilitates the high-speed information flow with an appropriate robustness in the network.

The clustering coefficient (C) is defined in terms of the connectivity of triple-node graphs and shows the mean probability that direct neighbours of two directly connected nodes are directly connected as well. It quantifies robustness of the brain network performance in information transmission. The higher value of C, the larger number of fully interconnected triple nodes and the higher robustness.

The mean path length of a graph (L) is the shortest path that exists between each node pairs averaged over all node pairs. The higher L is, the slower is information transmission among the nodes of the graph.

Therefore, the C and L values of the obtained graphs (for both normal and MA groups) were computed in the following way:

C is computed as follows (Stam et al., 2007):

$$C = \frac{1}{N}\sum_{i=1}^{N}\frac{\sum_{1\leqslant j<k\leqslant N} a_{ij}a_{jk}a_{ki}}{\sum_{1\leqslant j<k\leqslant N} a_{ij}a_{ik}}, \quad (1)$$

where a_{ij} is the weight of the edge connecting the ith node to the jth node and N is the number of nodes in the graph. Indeed, C, varying between 0 and 1, represents redundancy and quantifies how strongly the information is transmitted in the graph when some connections are disturbed (such as in the case of a brain disorder when neuronal areas do not function properly or their connections are dead). Indeed, it shows what portion of all triple combinations of nodes is fully connected.

L is considered a global quantification measure and is computed as follows (Latora and Marchiori, 2003; Li et al., 2007):

$$L = \frac{1}{N}\sum_{1\leqslant j<i\leqslant N}\left(\frac{1}{d_{ij}}\right), \quad (2)$$

where $d_{ij} = \frac{1}{a_{ij}}$ is defined as the inverse of the weight between ith and jth nodes.

The high ratio of C to L is the main characteristic of SW, as an SWN has high C and low L. Therefore, the C/L ratio was computed also to find out changes of the SW in MA abusers. In this way, the SW properties were computed in the normal subjects and the MA abusers based on both VGS and coherence methods.

2.4. Statistical analysis and classification

The Mann–Whitney statistical test was used to evaluate the differences of C, L and C/L between the normal and MA groups at each EEG sub-band. Then, using Pearson's coefficient of correlation, the dependence of daily dose, daily dose/body weight and lifetime use of MA with the obtained C, L and C/L was assessed. In order to show temporal stability of the discriminative features (in distinguishing the two groups), the EEGs were subdivided to four intervals and the ability of the features (obtained in each interval) in discriminating the two groups was analysed by repeated measures analysis of variance (ANOVA).

Moreover, in order to investigate the sources of differences between the two groups, extra analysis was carried out based on the demographic and behavioural factors in which the two groups were different. As such, at first using the median split method the healthy subjects were categorised into low- and high-level groups according to each factor. By this method, any value less than the median is categorised as low and any value higher than the median is categorised as high. Then, the differences of C/L between each pair-subgroup (low and high, according to each factor) were tested using Mann–Whitney tests.

Furthermore, machine classification was applied to differentiate the most discriminative C, L and C/L between the MA and normal groups, using Enhanced Probabilistic Neural Network (EPNN) (Ahmadlou and Adeli, 2010b). A repeated random sub-sampling cross-validation method was used for evaluation of the classification accuracy (Ahmadlou and Adeli, 2010a). As such, 2/3 of the data (data of 48 subjects) were randomly selected and used for training and the remaining data (data of 24 subjects) were used for testing. This random selection was repeated 100 times and the average value was considered as the final accuracy for discriminating the MA and normal groups.

3. Results

Table 1 shows the demographic and behavioural characteristics of the subjects. Compared with the normal subjects, the MA patients had higher level of stress (p-value <0.01) and depression (p-value <0.05). Further, there were only nine normal subjects using nicotine, whereas all of the MA abusers also used nicotine daily. The daily nicotine dose of the MA abusers was much more than that of the normal subjects who used the nicotine (p-value <0.01). There was also higher handedness and lower general intelligence in the MA group comparing to the normal group (p-value <0.05). There were no difference between the groups in age, weight and anxiety.

C, L and C/L of the VGS and coherence matrices in the normal and MA groups were computed at all the EEG sub-bands.

Fig. 2 depicts the results obtained by the VGS. Fig. 2a shows the mean C values for the normal (triangle) and MA (square) groups at the all sub-bands. The mean C values at all sub-bands in the MA group are greater than those in the normal group. The Mann–Whitney test showed that the difference of C values between the two groups is statistically significant in the gamma band (p-value <0.005), while the difference was not significant in the other frequency bands. Fig. 2b shows the mean L values for the normal (triangle) and MA (square) groups at the all sub-bands. The mean L values at all sub-bands in the MA group are less than those in the normal group. The L value at the gamma band in the MA group was significantly lower, compared with the normal group (p-value <0.005). There was no significant difference of the L values between the normal and MA groups in the other frequency bands. Fig. 2c shows the mean C/L values for the two groups at all the EEG sub-bands. The mean C/L values at all sub-bands in the MA group are higher compared with those of the normal group. The statistical analysis showed that the difference of C/L values between the two groups is significant in the gamma band (p-value <0.005), whereas the difference was not significant in the other bands. The mean and standard deviation of the C, L and C/L values, obtained by the VGS, are presented in Table 2.

Fig. 3 shows the results obtained by the magnitude square coherence. Likewise Fig. 3a–c, respectively, shows the mean C, L, and C/L values for the normal (triangle) and MA (square) groups at the all sub-bands. The obtained results by coherence were similar to the results by VGS. Fig. 3a shows that the mean C values in the MA group are higher than those in the normal group in all bands. The between-group difference of C values was significant only in the delta and gamma bands (p-value <0.05). Fig. 3b shows the reduced mean L values in the MA group at all bands; however,

Please cite this article in press as: Ahmadlou M et al. Global organization of functional brain connectivity in methamphetamine abusers. Clin Neurophysiol (2013), http://dx.doi.org/10.1016/j.clinph.2012.12.003

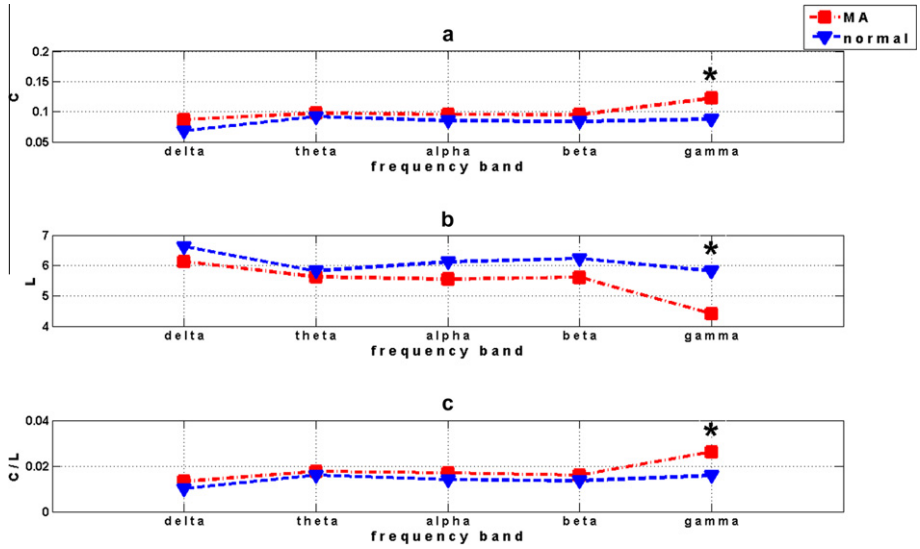

Fig. 2. Illustration of (a) *C*, (b) *L*, and (c) *C*/*L* of the VGS matrix in MA (square) and normal (triangle) groups at different frequency bands; *p-value <0.005.

Table 2
Mean and standard deviation of *C*, *L*, and *C*/*L* values, obtained by the VGS, in the EEG bands in the normal and MA groups.

	Characteristic	Normal		MA	
		M	Std	M	Std
Delta	*C*	.0685	.0402	.0868	.0603
	L	6.6176	1.4394	6.1270	1.4233
	C/*L*	.0100	.0051	.0132	.0067
Theta	*C*	.0917	.0691	.0972	.0852
	L	5.8204	2.0053	5.6176	1.4017
	C/*L*	.0160	.0086	.0176	.0100
Alpha	*C*	.0847	.0524	.0956	.0580
	L	6.1143	1.5165	5.5464	1.5084
	C/*L*	.0140	.0102	.0171	.0130
Beta	*C*	.0835	.0503	.0947	.0466
	L	6.2227	2.3897	5.6029	1.6979
	C/*L*	.0135	.0102	.0163	.0082
Gamma	*C*	.0873	.0324	.1223	.0395
	L	5.8150	1.6801	4.4004	1.3931
	C/*L*	.0158	.0098	.0260	.0112

M, mean; Std., standard deviation.

only in the gamma band was the difference significant (p-value <0.01). Fig. 3c shows that the mean *C*/*L* values at all sub-bands in the MA group are increased; however, the between-group difference of the *C*/*L* values was significant only in the gamma band (p-value <0.01). The mean and standard deviation of the *C*, *L* and C/*L* values, obtained by the magnitude square coherence, are presented in Table 3.

As compared to the coherence, the VGS showed more discriminative characteristics (in the gamma band), in distinguishing the MA and normal groups, and the *C*, *L* and *C*/*L* of the VGS matrix at the gamma band were considered as the inputs of the EPNN classifier to distinguish the normal and MA groups. The results showed an accuracy of 82.8% in discriminating the two groups with sensitivity and specificity of 85.1% and 78.9%, respectively. Also for the better comparison between the VGS and the coherence, the EPNN was used to discriminate the two groups based on the same features (*C*, *L* and *C*/*L* in the gamma band) obtained by the coherence. The obtained accuracy was 74.7%.

For evaluating the temporal stability of the phenomenon of the deficient SW in gamma-band brain networks in the MA abusers, the 80-s EEGs were subdivided to four separate 20-s intervals and the gamma-band SW characteristic (*C*/*L*) was computed in both MA abuser and healthy groups. Considering the interval (labelled int 1, 2, 3 and 4 in Fig. 4) as a within-subjects factor and the group (MA and normal) as a between-subjects, repeated-measures ANOVA was used. Both VGS and coherence confirmed the temporal stability of the phenomenon. For the VGS at the gamma band, the significant between-subjects p-value of 0.0001 ($F = 229.68$) and the insignificant within-subjects p-value of 0.132 ($F = 2.32$) were obtained. For the coherence at the gamma band, the between-subjects difference was significant with a p-value of 0.008 ($F = 63.27$) and the within-subjects p-value was insignificant at 0.091 ($F = 4.04$). Fig. 4a and b shows the mean (tick bar) and standard deviation (thin bar) of the *C*/*L* values obtained by the VGS and coherence, respectively, in the gamma band in the four intervals (int1, int2, int3, and int4, in the temporal order) in each group.

Further, there were no significant correlations between the daily dose, daily dose/body weight and lifetime use of MA and the *C*, *L* and *C*/*L* of the MA abusers in the gamma band, neither based on the coherence nor based on the VGS. Table 4 shows the associated Pearson correlation coefficients and p-values.

Please cite this article in press as: Ahmadlou M et al. Global organization of functional brain connectivity in methamphetamine abusers. Clin Neurophysiol (2013), http://dx.doi.org/10.1016/j.clinph.2012.12.003

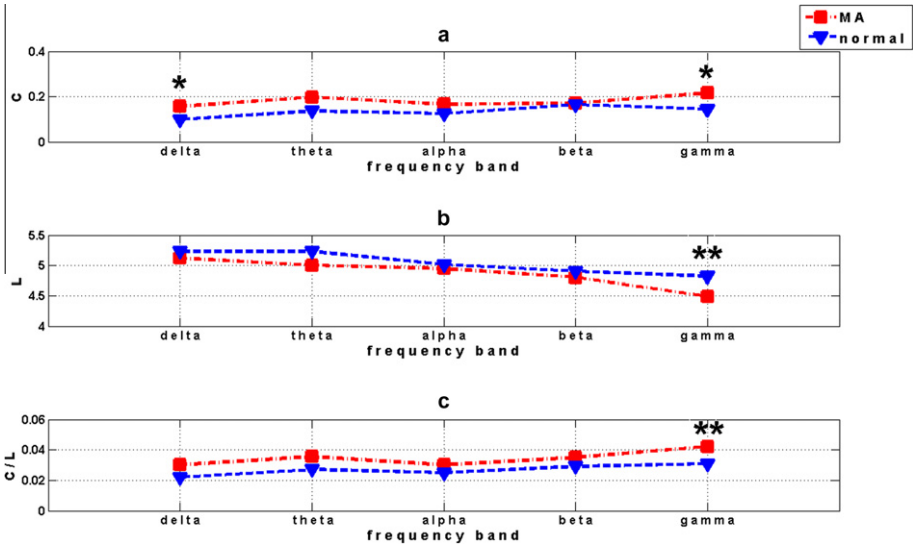

Fig. 3. Illustration of (a) *C*, (b) *L*, and (c) *C*/*L* of the coherence matrix in MA (square) and normal (triangle) groups at different frequency bands; $^{*}p$-value <0.05; $^{**}p$-value <0.01.

Table 3
Mean and standard deviation of *C*, *L*, and *C*/*L* values, obtained by the magnitude square coherence, in the EEG bands in the normal and MA groups.

	Characteristic	Normal		MA	
		M	Std	M	Std
Delta	*C*	.0985	.0755	.1568	.1085
	L	5.2276	.4058	5.1200	.5293
	C/*L*	.0221	.0192	.0302	.0198
Theta	*C*	.1356	.1097	.1972	.1583
	L	5.2294	.3932	5.0017	.4954
	C/*L*	.0272	.0176	.0356	.0184
Alpha	*C*	.1247	.1178	.1656	.1565
	L	5.0114	.4542	4.9464	.3261
	C/*L*	.0251	.0099	.0303	.0194
Beta	*C*	.1645	.1014	.1715	.1292
	L	4.9027	.3923	4.8029	.3618
	C/*L*	.0294	.0125	.0350	.0166
Gamma	*C*	.1443	.0949	.2153	.1290
	L	4.8240	.2463	4.9404	.2731
	C/*L*	.0308	.0147	.0421	.0169

M, mean; Std, standard deviation.

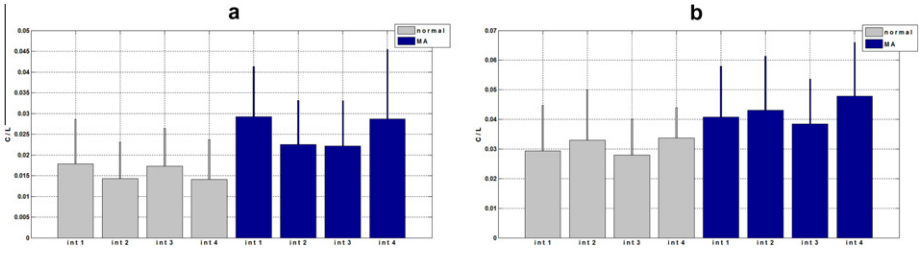

Fig. 4. Mean (tick bar) and standard deviation (thin bar) of the *C*/*L* values, obtained by (a) VGS and (b) coherence, in gamma in the four intervals (int1, int2, int3 and int4, in the temporal order) in each group (MA in blue and normal in gray). (For interpretation of the references to colour in this figure legend, the reader is referred to the web version of this article.)

Table 1 showed a significant difference between the handedness, general intelligence, daily nicotine dose stress and depression of the MA and normal groups, which may affect the SW of the brain at the gamma band, whether the subjects are MA or normal. In order to investigate the effects of the factors (i.e., handedness, general intelligence, stress, daily nicotine dose and depression) on the SW of the brain in the gamma band, the authors did two analyses: (1) the Pearson correlation was computed to see whether there is any correlation between each factor and the SW factor (*C*/*L*). Table 5 shows the Pearson correlation coefficients (and the associated *p*-values) between handedness, general intelligence, daily nicotine dose, stress and depression and the gamma band *C*/*L* obtained by the VGS in the MA and normal groups. There was a significant negative correlation between the general

Table 4
Results of correlations between daily dose, daily dose/body weight, and lifetime use of the methamphetamine and the *C*, *L*, and *C*/*L* of the MA abusers obtained by the VGS and coherence in gamma.

Measure	Characteristic	Daily dose	Lifetime dose	Daily dose/body weight
VGS	*C* Pearson corr. coef.	.12	.07	.11
	p-Value	NS	NS	NS
	L Pearson corr. coef.	−.20	.17	−.41
	p-Value	NS	NS	NS
	C/*L* Pearson corr. coef.	.02	.03	.02
	p-Value	NS	NS	NS
Coherence	*C* Pearson corr. coef.	.31	−.13	.24
	p-Value	NS	NS	NS
	L Pearson corr. coef.	−.19	.32	−.15
	p-Value	NS	NS	NS
	C/*L* Pearson corr. coef.	.28	−.08	.13
	p-Value	NS	NS	NS

Pearson corr. coef., Pearson correlation coefficient; NS, non-significant.

Table 5
Results of correlations between handedness, general intelligence, daily nicotine dose, stress and depression and the gamma band *C*/*L* obtained by the VGS in the MA and normal groups.

Measure	Characteristic		*C*/*L*
Normal	Handedness	Pearson corr. coef.	.12
	N = 36	*p*-Value	NS
	General intelligence	Pearson corr. coef.	−.21
	N = 36	*p*-Value	NS
	Daily nicotine dose	Pearson corr. coef.	−.15
	N = 9	*p*-Value	NS
	Stress	Pearson corr. coef.	.19
	N = 36	*p*-Value	NS
	Depression	Pearson corr. coef.	−.16
	N = 36	*p*-Value	NS
MA	Handedness	Pearson corr. coef.	−.10
	N = 36	*p*-Value	NS
	General intelligence	Pearson corr. coef.	−.63
	N = 36	*p*-Value	.04
	Daily nicotine dose	Pearson corr. coef.	.35
	N = 36	*p*-Value	NS
	Stress	Pearson corr. coef.	.07
	N = 36	*p*-Value	NS
	Depression	Pearson corr. coef.	.03
	N = 36	*p*-Value	NS

N, number of subjects; Pearson corr. coef., Pearson correlation coefficient; NS, non-significant.

intelligence and the gamma band *C*/*L* in the MA abusers (correlation coefficient = −0.63, *p*-value = 0.04), but not in the normal subjects. The other factors did not significantly correlate with the *C*/*L* (*p*-value >0.05), neither in the normal group nor in the MA group. (2) For each factor the normal group was divided into two subgroups with low and high scores (using the median split method) and then the difference of the *C*/*L* values, obtained by the VGS at the gamma band, in each pair-subgroup was tested using Mann–Whitney tests. Therefore, the comparisons of *C*/*L* values were accomplished separately between the low and high depressed normal subjects, between the normal subjects with low and high general intelligence, between the normal subjects with low stress and high stress, between the normal subjects with and without nicotine use and between with low and high scores in the handedness test. Table 6 represents the results of the subgroup analysis, including mean and standard deviation of the corresponding demographic/behavioural characteristics and the gamma band *C*/*L* values in each subgroup and the associated *p*-values in discrimination of the pair-subgroups. There were no significant difference of the gamma band *C*/*L* values in any pair-subgroups (*p*-value >0.2).

4. Discussion and conclusion

Although the worldwide MA abuse is increasing, only a few studies have investigated effects of chronic MA exposure on the human brain. As the global organization of the FC network of the brain plays an essential role in efficiency, synchronisability and robustness of the brain network, in this study the authors attempted to find out the effects of chronic MA abuse on the global organization of the FC brain network (in the framework of SW). FC was computed by both linear and nonlinear measures of

Table 6
Results of the subgroup analysis, including mean and standard deviation of the demographic/behavioural characteristics and the gamma band *C*/*L* and the associated *p*-values (of the gamma band *C*/*L*) in discrimination of each pair subgroup.

Sub-group		C/L M (S)	The corresponding demographic/ behavioural values M (S)	*p*-Value
Handedness	Low-level	.0146 (.0124)	62.77 (24.52), *N* = 18	.74
	High-level	.0165 (.0119)	92.80 (1.18), *N* = 18	
General intelligence	Low-level	.0144 (.0113)	113.37 (3.82), *N* = 18	.42
	High-level	.0184 (.0076)	122.83 (2.75), *N* = 18	
Daily nicotine dose	Low-level	.0153 (.0088)	0 (0), *N* = 9	.46
	High-level	.0127 (.0086)	2.75 (1.78), *N* = 9	
Stress	Low-level	.0152 (.0106)	3.20 (3.05), *N* = 18	.20
	High-level	.0105 (.0084)	10.34 (1.69), *N* = 18	
Depression	Low-level	.0156 (.0092)	3.81 (5.59), *N* = 18	.44
	High-level	.0185 (.0104)	13.54 (3.91), *N* = 18	

M, mean; S, standard deviation; *N*, number of subjects.

Please cite this article in press as: Ahmadlou M et al. Global organization of functional brain connectivity in methamphetamine abusers. Clin Neurophysiol (2013), http://dx.doi.org/10.1016/j.clinph.2012.12.003

synchronization. The nonlinear method was VGS (Ahmadlou and Adeli, 2012b) and magnitude coherence was used as the linear method. As the strength of the FC in different frequencies may be affected by the distances between the neuronal regions (FC in the higher (lower) frequencies are appeared usually between the shorter- (longer-) distant regions), the Small-World properties (the C and L) were analysed in different frequency bands. To the best of the authors' knowledge, this is the first study on deficits of the global organization of brain networks in the MA abusers.

Except a small between-group difference of the C at delta, obtained by the coherence, the other differences between normal and MA abuser groups were found only at the EEG gamma band, and not at the other EEG bands. Moreover, the VGS showed more significant differences (smaller p-values) between the two groups in the gamma band. Gamma frequency is the band most reactive to cognitive information binding and processing (Herrmann and Demiralp, 2005; Fries, 2009; Wilson et al., 2012). Therefore, the obtained differences in the gamma band of the MA abusers may implicate their cognitive deficits; the significant correlation between the gamma band C/L and the general intelligence in the MA abusers is an evidence to support this hypothesis. In the gamma band the results showed greater C and lower L in the MA abusers, compared to the normal group, which indicate the higher number of closed-loop triple connections (the locally intertwined connections) and the shorter path lengths over all the brain network, respectively. The higher C/L in MA abusers implies a global hypersynchronization in the short-distant FC over all the brain in the gamma frequency range. In this view, the obtained results accord with the central neural system hyper-excitability in abstinent alcoholics reported by Begleiter and Porjesz (1977). This hyper-excitability was attributed by the researchers to the withdrawal effects of alcohol (Begleiter and Porjesz, 1977, 1999). After the stage of withdrawal, abstinent alcoholics (and drug abusers) generally display signs of reduced brain function and cognition, such as smaller-than-normal amplitude of the P300 components of the ERP (Porjesz et al., 1987; Realmuto et al., 1993; Ji et al., 1999; Hada et al., 2000; Jones et al., 2006), reduced regional cerebral blood flow (Berglund et al., 1989) and positron emission tomography (PET) imaging of reduced dopamine receptor activity, especially in the striatum, (Volkow et al., 2006) even after prolonged abstinence from the substance. The abstinent MA abusers show also the similar signs, such as abnormal regional cerebral glucose metabolism (London et al., 2004), reduced regional cerebral blood flow (Chang et al., 2005; Hwang et al., 2006), enlargement of the basal ganglia and white matter volumes (detected by magnetic resonance imaging, MRI), reduced brain dopamine transporters during short abstinence (<6 months), especially in the striatum (detected by PET imaging) and reduced cognitive performance during the early abstinence (Chang et al., 2007). Hence, the fact that in the current study the patients were in the withdrawal stage (1–3 weeks) is of great importance and indeed the obtained findings may reflect the withdrawal effects from MA. However, as MA induces depression in GABA(B) receptor signalling (Padgett et al., 2012) and depressing or blocking the GABA(B) receptors results in increasing gamma waves (Leung and Shen, 2007), the abnormality of SW in the gamma band may reflect the chronic exposure to MA and not the abstinence. Therefore, it is not clear whether the current findings reflect the abstinence effects or the chronic exposure to MA.

The high accuracy of the EPNN in the discrimination of the two groups showed the high potential of the SW properties of the FC brain network at the gamma band in diagnosis of the MA abusers. Moreover, as genetics plays a significant role in alcoholism and drug abuse, this finding could be a vulnerability marker (antecedent instead of consequence) that can also be found before the onset of the MA abuse, as has been found in alcoholism and schizophrenia (Rangaswamy et al., 2004; Dick et al., 2006; Rangaswamy and Porjesz, 2008). Therefore, the capability of the current finding in prediction of MA abuse would be examined in future studies of the authors.

So far, only two studies have investigated the changes of the resting-state brain electrical activities in human MA abusers (Newton et al., 2003, 2004). They recorded the resting EEGs for at least 20 min and found that MA abusers possess increased EEG powers in low frequencies, while we did not find any differences in the Small-World properties in the low frequencies (except for the small difference in C at the delta band, obtained by the coherence). As the authors did not use EOG electrodes, the low-frequency activities could be affected by eye blinking or eye-artefacts. Further, their long time of recording might induce fatigue, which increases the low frequency waves (Tanaka et al., 2012). The between-group difference in the C at the delta band, obtained by the coherence in this study, might indicate the difference of slow wave reported in their study. However, as there is no direct relationship between the power spectrum analysis (which they did) and the global organization analysis of the FC of the brain presented in the current study, a clear link or conflict between the results could not be inferred. Further, unfortunately, as they have analysed the EEGs only between 0.5 and 20 Hz, there is no finding regarding changes of gamma activity in previous human studies. However, the deficient topology at the gamma band in the FC brain network of the MA abusers observed in this study accords with the higher gamma activity observed in animals (mouse and monkey) with MA or amphetamine exposure (Pinault, 2008; Morra et al., 2012). In addition, as recent studies have strongly shown that the inhibitory interneurons (especially fast-spiking Parvalbumin-positive neurons) are responsible to generate gamma activity (Traub et al., 2001; Bartos et al., 2007; Cardin et al., 2009) and as MA causes a major deficit on the dopaminergic and serotonergic system (Nordahl et al., 2003; Belcher et al., 2009; De La Garza et al., 2010), this finding may implicitly imply on the effects of the deficient dopaminergic and serotonergic system on the fast-spiking inhibitory neurons.

Overall, this was a quasi-experimental study and as a human study there were some intrinsic limitations from matching the behavioural and demographic characteristics of the two groups due to unavailability of backgrounds of the subjects. Hence, more pure studies using genetically modified animals with better control matching are necessary to support the obtained findings in this study.

Conflicts of interest

The authors have no conflicts of interest to disclose.

Acknowledgement

Many thanks go to the reviewers for their effective comments and helpful advice in the revision procedure.

Appendix A. Computation of visibility graph similarity (Ahmadlou and Adeli, 2012b)

The visibility graph (VG) algorithm converts a time series to a graph keeping the order of the VG nodes the same as the order of sample times of the time series (Lacasa et al., 2008). It is shown that the topology of the VG of a time series inherits dynamical properties of the time series, such as complexity and fractality. The visibility graph similarity (VGS) quantifies the interdependencies between two (or more) time series based on similarity of the

VGs to their reconstructed trajectories in a state space. Briefly, the VGS of two time series is computed in the following way:

(a) Each time series is recontructed as a trajectory in a state space.
(b) For each trajectory, a distance time series (DTS) is created from a sequence of relative distances of the states to a reference state.
(c) The VG of each trajectory is constructed using the obtained DTS. Then, a sequence of degrees (the degree of a node is the number of edges connected to that node) of the VG (called the degree sequence, DS) is obtained.
(d) Correlation of the two DSs is computed, which is called the VGS between the two time series.

Appendix B. Computation of magnitude square coherence (Carter et al., 1973)

Magnitude square coherence is a conventional measure of linear synchronization developed by Carter et al. (1973). Given the signals x and y, the coherence between them is computed in the following way:

(a) x and y are subdivided in N segments of the same length.
(b) For each segment, $X(f)$ and $Y(f)$, the Fourier transforms of x and y, respectively, are computed (where f indicates frequency).
(c) The magnitude square coherence between x and y, $c(f)$, is computed as:

$$c(f) = \frac{|\langle X(f)Y^*(f)\rangle|^2}{|\langle X(f)\rangle||\langle Y(f)\rangle|}, \quad \text{(B1)}$$

where $< X(f) >$ indicates the averaged $X(f)$ overall the N segments. $|X(f)|$ and $X^*(f)$ indicate magnitude and complex conjugate of $X(f)$, respectively.

References

Ahmadlou M, Adeli H. Wavelet-synchronization methodology: a new approach for EEG-based diagnosis of ADHD. Clin EEG Neurosci 2010a;41:1–10.
Ahmadlou M, Adeli H. Enhanced probabilistic neural network with local decision circles: a robust classifier. Integr Comput Aided Eng 2010b;17:197–210.
Ahmadlou M, Adeli H. Functional community analysis of brain: a new approach for EEG-based investigation of the brain pathology. Neuroimage 2011;58:401–8.
Ahmadlou M, Adeli H. Visibility graph similarity: a new measure of generalized synchronization in coupled dynamic systems. Physica D 2012;241:326–32.
Ahmadlou M, Adeli H, Adeli A. Graph theoretical analysis of organization of functional brain networks in ADHD. Clin EEG Neurosci 2012a;43:5–13.
Ahmadlou M, Rostami R, Sadeghi V. Which attention-deficit/hyperactivity disorder children will be improved through neurofeedback therapy? A graph theoretical approach to neocortex neuronal network of ADHD. Neurosci Lett 2012b;516:156–60.
Ahmadlou M, Adeli H, Adeli A. Improved visibility graph fractality with application for the diagnosis of autism spectrum disorder. Physica A 2012c;391:4720–6.
Ahmadlou M, Adeli H, Adeli A. Fractality analysis of frontal brain in major depressive disorder. Int J Psychophysiol 2012d;85:206–11.
Ahmadlou M, Adeli H, Adeli A. Fuzzy synchronization likelihood-wavelet methodology for diagnosis of autism spectrum disorder. J Neurosci Methods 2012e;211:203–9.
Bae SC, Lyoo IK, Sung YH, Yoo J, Chung A, Yoon S-J, et al. Increased white matter hyperintensities in male methamphetamine abusers. Drug Alcohol Depend 2006;81:83–8.
Bartos M, Vida I, Jonas P. Synaptic mechanisms of synchronized gamma oscillations in inhibitory interneuron networks. Nat Rev Neurosci 2007;8:45–56.
Bassett DS. Small-world brain networks. Neuroscientist 2006;12:512–23.
Begleiter H, Porjesz B. Persistence of brain hyperexcitability following chronic alcohol exposure in rats. Adv Exp Med Biol 1977;85B:209–22.
Begleiter H, Porjesz B. What is inherited in the predisposition toward alcoholism? A proposed model. Alcohol Clin Exp Res 1999;23:1125–35.
Belcher AM, O'Dell SJ, Marshall JF. Long-term changes in dopamine-stimulated gene expression after single-day methamphetamine exposure. Synapse 2009;63:403–12.
Berglund M, Prohovnik I, Risberg J. Regional cerebral blood flow during alcoholic blackout. Psychiatry Res 1989;27:49–54.
Cardin JA, Carlén M, Meletis K, Knoblich U, Zhang F, Deisseroth K, et al. Driving fast-spiking cells induces gamma rhythm and controls sensory responses. Nature 2009;459:663–7.
Carter GC, Knapp CH, Nuttall AH. Estimation of the magnitude-squared coherence function via overlapped fast Fourier transform processing. IEEE Trans Audio Electroacoust 1973;21:337–44.
Chang L, Alicata D, Ernst T, Volkow N. Structural and metabolic brain changes in the striatum associated with methamphetamine abuse. Addiction 2007;102:16–32.
Chang L, Cloak C, Patterson K, Grob C, Miller EN, Ernst T. Enlarged striatum in abstinent methamphetamine abusers: a possible compensatory response. Biol Psychiatry 2005;57:967–74.
Dauwels J, Vialatte F, Musha T, Cichocki A. A comparative study of synchrony measures for the early diagnosis of Alzheimer's disease based on EEG. Neuroimage 2010;49:668–93.
De La Garza II R, Zorick T, London ED, Newton TF. Evaluation of modafinil effects on cardiovascular, subjective, and reinforcing effects of methamphetamine in methamphetamine-dependent volunteers. Drug Alcohol Depend 2010;106:173–80.
Dick DM, Jones K, Saccone N, Hinrichs A, Wang JC, Goate A, et al. Endophenotypes successfully lead to gene identification: results from the collaborative study on the genetics of alcoholism. Behav Genet 2006;36:112–26.
Feil J, Sheppard D, Fitzgerald PB, Yücel M, Lubman DI, Bradshaw JL. Addiction, compulsive drug seeking, and the role of frontostriatal mechanisms in regulating inhibitory control. Neurosci Biobehav Rev 2010;35:248–75.
Fries P. Neuronal gamma-band synchronization as a fundamental process in cortical computation. Annu Rev Neurosci 2009;32:209–24.
Glasner-Edwards S, Mooney LJ, Marinelli-Casey P, Hillhouse M, Ang A, Rawson R. Clinical course and outcomes of methamphetamine-dependent adults with psychosis. J Subst Abuse Treat 2008;35:445–50.
Hada M, Porjesz B, Begleiter H, Polich J. Auditory P3a assessment of male alcoholics. Biol Psychiatry 2000;48:276–86.
Henry BL, Minassian A, Perry W. Effect of methamphetamine dependence on everyday functional ability. Addict Behav 2010;35:593–8.
Herrmann CS, Demiralp T. Human EEG gamma oscillations in neuropsychiatric disorders. Clin Neurophysiol 2005;116:2719–33.
Hjorth B. An on line transformation of EEG scalp potentials into orthogonal source derivations. Electroencephalogr Clin Neurophysiol 1975;39:526–30.
Hwang J, Lyoo IK, Kim SJ, Sung YH, Bae S, Cho SN, et al. Decreased cerebral blood flow of the right anterior cingulate cortex in long-term and short-term abstinent methamphetamine users. Drug Alcohol Depend 2006;82:177–81.
Iudicello JE, Weber E, Grant I, Weinborn M, Woods SP. HIV Neurobehavioral Research Center Group. Misremembering future intentions in methamphetamine-dependent individuals. Clin Neuropsychol 2012;25:269–86.
Ji J, Porjesz B, Begleiter H. Event-related potential index of semantic mnemonic dysfunction in abstinent alcoholics. Biol Psychiatry 1999;45:494–507.
Jones KA, Porjesz B, Chorlian D, Rangaswamy M, Kamarajan C, Padmanabhapillai A, et al. S-transform time-frequency analysis of P300 reveals deficits in individuals diagnosed with alcoholism. Clin Neurophysiol 2006;117:2128–43.
Kalechstein AD, De la Garza R, Newton TF, Green MF, Cook IA, Leuchter AF. Quantitative EEG abnormalities are associated with memory impairment in recently abstinent methamphetamine-dependent individuals. J Neuropsychiatry Clin Neurosci 2009;21:254–8.
Lacasa L, Luque B, Ballesteros F, Luque J, Nuno JC. From time series to complex networks: the visibility graph. Proc Natl Acad Sci U S A 2008;105:4972–5.
Latora V, Marchiori M. Economic small-world behavior in weighted networks. European Physical Journal B 2003;32:249–63.
Leung LS, Shen B. GABAB receptor blockade enhances theta and gamma rhythms in the hippocampus of behaving rats. Hippocampus 2007;17:281–91.
Li W, Lin Y, Liu Y. The structure of weighted small-world networks. Physica A 2007;376:708–18.
Liu Y, Liang M, Zhou Y, He Y, Hao Y, Song M, et al. Disrupted small-world networks in schizophrenia. Brain 2008;131:945–61.
London ED, Simon SL, Berman SM, Mandelkern MA, Lichtman AM, Bramen J, et al. Mood disturbances and regional cerebral metabolic abnormalities in recently abstinent methamphetamine abusers. Arch Gen Psychiatry 2004;61:73–84.
Ma S, Calhoun VD, Eichele T, Du W, Adali T. Modulations of functional connectivity in the healthy and schizophrenia groups during task and rest. Neuroimage 2012;62:1694–704.
Mahajan Y, McArthur G. Does combing the scalp reduce scalp electrode impedances? J Neurosci Methods 2010;188:287–9.
Mamashli F, Ahmadlu M, Golpayegani MR, Gharibzadeh S. Detection of attention using chaotic global features. J Neuropsychiatry Clin Neurosci 2010;22:e20.
Maxwell JC, Brecht M-L. Methamphetamine: here we go again? Addict Behav 2011;36:1168–73.
Morra JT, Glick SD, Cheer JF. Cannabinoid receptors mediate methamphetamine induction of high frequency gamma oscillations in the nucleus accumbens. Neuropharmacology 2012;63:565–74.
Newton TF, Cook IA, Kalechstein AD, Duran S, Monroy F, Ling W, et al. Quantitative EEG abnormalities in recently abstinent methamphetamine dependent individuals. Clin Neurophysiol 2003;114:410–5.
Newton TF, Kalechstein AD, Hardy DJ, Cook IA, Nestor L, Ling W, et al. Association between quantitative EEG and neurocognition in methamphetamine dependent volunteers. Clin Neurophysiol 2004;115:194–8.

Please cite this article in press as: Ahmadlou M et al. Global organization of functional brain connectivity in methamphetamine abusers. Clin Neurophysiol (2013), http://dx.doi.org/10.1016/j.clinph.2012.12.003

Nordahl TE, Salo R, Leamon M. Neuropsychological effects of chronic methamphetamine use on neurotransmitters and cognition. J Neuropsychiatry Clin Neurosci 2003;15:317–25.

Padgett CL, Lalive AL, Tan KR, Terunuma M, Munoz MB, Pangalos MN, et al. Methamphetamine-evoked depression of GABA(B) receptor signaling in GABA neurons of the VTA. Neuron 2012;73:978–89.

Park C-H, Kim SY, Kim Y-H, Kim K. Comparison of the small-world topology between anatomical and functional connectivity in the human brain. Physica A 2008;387:5958–62.

Pinault D. NMDA receptor antagonists ketamine and MK-801 induce wake-related aberrant gamma oscillations in the rat neocortex. Biol Psychiatry 2008;63:730–5.

Polesskaya O, Silva J, Sanfilippo C, Desrosiers T, Sun A, Shen J, et al. Methamphetamine causes sustained depression in cerebral blood flow. Brain Res 2011;1373:91–100.

Porjesz B, Begleiter H, Bihari B, Kissin B. Event-related brain potentials to high incentive stimuli in abstinent alcoholics. Alcohol 1987;4:283–7.

Raven J. The Raven's progressive matrices: change and stability over culture and time. Cognit Psychol 2000;41:1–48.

Rangaswamy M, Porjesz B. Uncovering genes for cognitive (dys)function and predisposition for alcoholism spectrum disorders: a review of human brain oscillations as effective endophenotypes. Brain Res 2008;1235: 153–71.

Rangaswamy M, Porjesz B, Chorlian DB, Wang K, Jones KA, Kuperman S, et al. Resting EEG in offspring of male alcoholics: beta frequencies. Int J Psychophysiol 2004;51:239–51.

Realmuto G, Begleiter H, Odencrantz J, Porjesz B. Event-related potential evidence of dysfunction in automatic processing in abstinent alcoholics. Biol Psychiatry 1993;33:594–601.

Schwartz DL, Mitchell AD, Lahna DL, Luber HS, Huckans MS, Mitchell SH, et al. Global and local morphometric differences in recently abstinent methamphetamine-dependent individuals. Neuroimage 2010;50:1392–401.

Silber B, Croft R, Camfield DA, Downey LA, Papafotiou K, Stough C. The acute effects of D-amphetamine and D-methamphetamine on ERP components in humans. Eur Neuropsychopharmacol 2012;22:492–500.

Sporns O, Zwi JD. The small world of the cereb cortex. Neuroinformatics 2004;2:145–62.

Sporns O, Chialvo DR, Kaiser M, Hilgetag CC. Organization, development and function of complex brain networks. Trends Cogn Sci 2004;8:418–25.

Stam CJ, Jones BF, Nolte G, Breakspear M, Scheltens P. Small-world networks and functional connectivity in Alzheimer's disease. Cereb Cortex 2007;17: 92–9.

Tanaka M, Shigihara Y, Ishii A, Funakura M, Kanai E, Watanabe Y. Effect of mental fatigue on the central nervous system: an electroencephalography study. Behav Brain Funct 2012;8:48.

Tandonnet C, Burle B, Hasbroucq T, Vidal F. Spatial enhancement of EEG traces by surface Laplacian estimation: comparison between local and global methods. Clin Neurophysiol 2005;116:18–24.

Thompson PM, Hayashi KM, Simon SL, Geaga JA, Hong MS, Sui Y, et al. Structural abnormalities in the brains of human subjects who use methamphetamine. J Neurosci 2004;24:6028–36.

Tobias MC, O'Neill J, Hudkins M, Bartzokis G, Dean AC, London ED. White-matter abnormalities in brain during early abstinence from methamphetamine abuse. Psychopharmacology 2010;209:13–24.

Traub RD, Kopell N, Bibbig A, Buhl EH, LeBeau FE, Whittington MA. Gap junctions between interneuron dendrites can enhance synchrony of gamma oscillations in distributed networks. J Neurosci 2001;21:9478–86.

Volkow ND, Wang GJ, Begleiter H, Porjesz B, Fowler JS, Telang F, et al. High levels of dopamine D2 receptors in unaffected members of alcoholic families: possible protective factors. Arch Gen Psychiatry 2006;63:999–1008.

Wang J, Zuo X, Dai Z, Xia M, Zhao Z, Zhao X, et al. Disrupted functional brain connectome in individuals at risk for Alzheimer's disease. Biol Psychiatry, in press. http://dx.doi.org/10.1016/j.biopsych.2012.03.026.

Watts DJ, Strogatz SH. Collective dynamics of 'small-world' networks. Nature 1998;393:409–10.

Wilson TW, Wetzel MW, White ML, Knott NL. Gamma-frequency neuronal activity is diminished in adults with attention-deficit-hyperactivity disorder: a pharmaco-MEG study. J Psychopharmacol 2012;26:771–7.

Yu S, Huang D, Singer W, Nikolić D. A small world of neuronal synchrony. Cereb Cortex 2008;18:2891–901.

Yuan K, Qin W, Liu J, Guo Q, Dong M, Sun J, et al. Altered small-world brain functional networks and duration of heroin use in male abstinent heroin-dependent individuals. Neurosci Lett 2010;477:37–42.

Zhang J, Wang J, Wu Q, Kuang W, Huang X, He Y, et al. Disrupted brain connectivity networks in drug-naive, first-episode major depressive disorder. Biol Psychiatry 2011;70:334–42.

Please cite this article in press as: Ahmadlou M et al. Global organization of functional brain connectivity in methamphetamine abusers. Clin Neurophysiol (2013), http://dx.doi.org/10.1016/j.clinph.2012.12.003